

Spontaneous \mathcal{PT} symmetry breaking in Dirac-Kronig-Penney crystals

Stefano Longhi

Dipartimento di Fisica, Politecnico di Milano, and Istituto di Fotonica e Nanotecnologie—Consiglio Nazionale delle Ricerche, Piazza Leonardo da Vinci 32, IT-20133 Milano, Italy

Francesco Cannata

Istituto Nazionale di Fisica Nucleare, Sezione di Bologna, IT-40127 Italy

Alberto Ventura

Italian National Agency for New Technologies, Centro Ricerche Ezio Clementel, Bologna, Italy, and Istituto Nazionale di Fisica Nucleare, Sezione di Bologna, IT-40129 Italy

(Received 8 September 2011; revised manuscript received 7 November 2011; published 21 December 2011)

We introduce a non-Hermitian \mathcal{PT} invariant extension of the Dirac-Kronig-Penney model, describing the motion of a Dirac quasiparticle in a locally periodic sequence of imaginary δ -Dirac barriers and wells, and propose its optical realization using superstructure fiber Bragg gratings with alternating regions of optical gain and absorption. For the infinite crystal, we determine the band structure and show that the \mathcal{PT} phase is always broken. For a finite crystal, we derive analytical expressions for reflection and transmission probabilities, and show that the \mathcal{PT} phase is unbroken below a finite threshold of the δ -barrier area. In the proposed optical realization, the onset of \mathcal{PT} symmetry breaking in the finite crystal corresponds to the lasing condition for the grating superstructures.

DOI: [10.1103/PhysRevB.84.235131](https://doi.org/10.1103/PhysRevB.84.235131)

PACS number(s): 71.20.-b, 71.15.Rf, 03.65.Nk, 03.65.Pm

I. INTRODUCTION

The Kronig-Penney (KP) model,¹ describing the band structure of an electron in an ideal one-dimensional crystal, has been widely regarded as a standard reference model in solid-state physics for more than half a century. The KP model has served on many occasions as a paradigmatic model to study at a basic level important physical phenomena, including band-structure properties, localization effects in disordered lattices, electronic properties of superlattices, and Peierls transitions. Since the (quasi)particles addressed in condensed-matter systems are typically nonrelativistic, the KP model has been more often considered for the Schrödinger equation. Relativistic extensions of the KP model [also referred to as the Dirac-Kronig-Penney (DKP) model²] have been introduced long ago as well (see, for instance, Refs. 2–5 and references therein). Earlier works on the DKP model were mainly focused on the study of the impact of relativity on the band structure and on localization phenomena, such as the shrinkage of the bulk bands with increasing band number. Photonic analogs of the DKP model, based on light scattering in superstructure optical Bragg gratings,⁶ have been also recently proposed by one of the present authors in Ref. 7. In such previous works, the main aim was to provide experimentally accessible classical simulators of the physics of relativistic ordinary crystals, offering the possibility to observe, e.g., relativistic band shrinkage or relativistic Tamm surface states. In the past recent years, the motion of relativistic Dirac particles in periodic potentials has seen a significant and renewed interest because the quasiparticles in honeycomb lattices, such as electrons in graphene,^{8,9} cold atoms in optical lattices,¹⁰ ultracold atoms in a light-induced gauge field,¹¹ trapped ions,¹² and light waves in photonic lattices,^{13,14} may be described in the framework of the relativistic Dirac equation. In particular, DKP models have been recently introduced and investigated

by several authors to study electron transport in graphene with applied periodic potentials.¹⁵ In such DKP models, the underlying periodic potential is real and the electron dynamics is governed by an Hermitian Hamiltonian. In recent years, an increasing attention has been devoted to investigating the band structure and transport properties of *complex crystals*, i.e., a kind of metamaterials in which the underlying periodic potential is complex valued (see, for instance, Refs. 16–23 and references therein). Early works on complex crystals^{16,17} were framed in the context of non-Hermitian extensions of nonrelativistic quantum mechanics²⁴ and were mainly regarded as curious mathematical models. In particular, a nonrelativistic KP model for a complex crystal was proposed in Ref. 17, in which an unusual band structure was found. Since the recent proposals and demonstrations of complex periodic potentials using matter¹⁸ or optical waves,¹⁹ culminating in the first experimental demonstration of parity-time (\mathcal{PT}) symmetric breaking in an optical directional coupler,²⁵ the study of complex crystals has gained a renewed interest. Complex crystals exhibit rather unique and distinct scattering and transport properties as compared to ordinary crystals, such as the violation of the Friedel's law of Bragg scattering,^{18,20} double refraction and nonreciprocal diffraction,¹⁹ anomalous transport,²¹ and unidirectional invisibility.²³ Like for scattering in complex barrier potentials, unitarity is generally lost and reflection probabilities are distinct for the two incidence sides.²⁶ Hence, they can be regarded as a kind of novel metamaterials. Exact results of \mathcal{PT} symmetry breaking in complex crystals have been recently presented in Refs. 27 and 28 using a tight-binding dimer lattice model with spatially separated gain and loss regions. In such works, it was suggested that symmetry breaking can be suppressed for binary modulation of distances between gain and loss regions. The possibility of simulating in optical structures the scattering of

relativistic particles from a complex potential barrier or well has been discussed in Ref. 29. In that work, it was shown that light propagation in a distributed-feedback optical structure with loss and/or gain regions mimics the evolution of the Dirac spinor wave function in a complex potential. The analysis of Ref. 29 was limited to considering relativistic scattering from single complex potential “wells” or “barriers,” highlighting the existence of two distinct types of spectral singularities and discussing their physical meaning. However, the physics and symmetry breaking properties of *periodic* and *complex* potentials in the framework of a relativistic wave equation were not investigated in such a preliminary work.

In this paper we propose a *relativistic* Kronig-Penney model of a complex crystal with \mathcal{PT} invariance, which provides a simple and exactly solvable model describing the dynamics of Dirac quasiparticles in a periodic sequence of alternating imaginary δ -Dirac barriers and wells. The main results of our analysis can be summarized as follows: (i) for the infinite DKP crystal the \mathcal{PT} phase is always broken and (ii) for a finite crystal containing a number N of unit cells the \mathcal{PT} phase is unbroken below a finite threshold of the δ -barrier area, which scales as $\sim 1/N$. The former result, which is rigorously proved by a perturbative analysis of the band dispersion curve of the DKP crystal, is a nontrivial result that shows that, as opposed to other exactly solvable models of \mathcal{PT} symmetric crystals (like the sinusoidal \mathcal{PT} symmetric crystal^{19,20}), for the complex extension of the DKP model the \mathcal{PT} phase is always broken. The latter result provides an important scaling law defining the dependence of the unbroken \mathcal{PT} phase on the number N of crystal cells.

II. \mathcal{PT} SYMMETRIC DIRAC-KRONIG-PENNEY MODEL AND ITS OPTICAL REALIZATION

A. The model

We consider the motion of a Dirac particle in a one-dimensional locally periodic system whose elementary cell of size $2d = 2(a + b)$ consists of an imaginary well of depth $-iV_1$ and width a and an imaginary barrier of height iV_1 and

width a , separated by a distance b [see Fig. 1(a)]. Note that in the $b \rightarrow 0$ limit the elementary cell reduces to a \mathcal{PT} symmetric barrier,³⁰ whereas when $a \rightarrow 0$ and $V_1 \rightarrow \infty$, with $aV_1 = Q$ a finite number, it reduces to a \mathcal{PT} symmetric combination of Dirac delta functions. Owing to the boundary conditions that will be imposed to the system, it is convenient to solve the time-independent one-dimensional Dirac equation with a scalar potential $S(x)$ and a vector potential $V(x)$:

$$E\psi(x) = -i\alpha_x \frac{\partial \psi}{\partial x} + \beta m(x)\psi(x) + V(x)\psi(x) \equiv \hat{H}\psi, \quad (1)$$

in the Weyl representation (see, for instance, Ref. 31):

$$\alpha_x = \sigma_z = \begin{pmatrix} 1 & 0 \\ 0 & -1 \end{pmatrix}, \quad \beta = \sigma_x = \begin{pmatrix} 0 & 1 \\ 1 & 0 \end{pmatrix}, \quad (2)$$

where $m(x) = m + S(x)$, m is the particle rest mass, and $\psi(x) = (\psi_1, \psi_2)^T$ is the two-component spinor wave function. In the following, we will consider either the infinite periodic crystal or a finite crystal composed by a number N of cells. In both cases, the band-structure and scattering properties of the crystal are mainly determined by the elements of the 2×2 transfer matrix of the unit cell, $\mathcal{M}^{(\text{cell})}(E)$, that relates the wave function $\psi(x)$ at the input ($x = 0$) and output ($x = 2d$) planes of the unit cell (see, for instance, Ref. 32). It is worth remarking that there is an alternative definition of the transfer matrix, which connects the two-dimensional vector of the coefficients of $\psi(2d)$ with the corresponding vector of $\psi(0)$ (see, for instance, Ref. 31). The two definitions of the transfer matrix are obviously related in a simple way. For stepwise constant values of $V(x)$ and $S(x)$, as in the DKP model, the transfer matrix can be calculated analytically as the cascading of the transfer matrices of each slice in which both $m(x)$ and $V(x)$ are constants. For the unit cell shown in Fig. 1(a) and assuming $m(x) = m$ (i.e., $S = 0$ inside the crystal), one can readily calculate the transfer matrix $\mathcal{M}^{(\text{cell})}(E)$ as the ordered product

$$\mathcal{M}^{(\text{cell})}(E) = \mathcal{M}_0(E)\mathcal{M}_+(E)\mathcal{M}_0(E)\mathcal{M}_-(E), \quad (3)$$

where

$$\mathcal{M}_0(E) = \begin{pmatrix} \cosh(\rho b) + i(E/\rho) \sinh(\rho b) & -i(m/\rho) \sinh(\rho b) \\ i(m/\rho) \sinh(\rho b) & \cosh(\rho b) - i(E/\rho) \sinh(\rho b) \end{pmatrix}, \quad (4)$$

$$\mathcal{M}_{\pm}(E) = \begin{pmatrix} \cosh(\rho_{\pm} a) + i(\sigma_{\pm}/\rho_{\pm}) \sinh(\rho_{\pm} a) & -i(m/\rho_{\pm}) \sinh(\rho_{\pm} a) \\ i(m/\rho_{\pm}) \sinh(\rho_{\pm} a) & \cosh(\rho_{\pm} a) - i(\sigma_{\pm}/\rho_{\pm}) \sinh(\rho_{\pm} a) \end{pmatrix} \quad (5)$$

are the transfer matrices of the various sections of the unit cell shown in Fig. 1(a), and where

$$\sigma_{\pm} = E \mp iV_1, \quad \rho = \sqrt{m^2 - E^2}, \quad \rho_{\pm} = \sqrt{m^2 - \sigma_{\pm}^2}. \quad (6)$$

Note that $\mathcal{M}^{(\text{cell})}(E)$ is a unimodular matrix, i.e., $\det \mathcal{M}^{(\text{cell})} = \mathcal{M}_{11}\mathcal{M}_{22} - \mathcal{M}_{12}\mathcal{M}_{21} = 1$. A particularly simple expression of $\mathcal{M}^{(\text{cell})}$ is obtained in the δ -Dirac limit of the

barrier and well. In fact, in the limit $V_1 \rightarrow \infty$, $a \rightarrow 0$ with $V_1 a = Q$ a finite number, one simply has

$$\mathcal{M}_{\pm} = \begin{pmatrix} \exp(\pm Q) & 0 \\ 0 & \exp(\mp Q) \end{pmatrix}. \quad (7)$$

Substitution of Eqs. (4) and (7) into Eq. (3) yields the following explicit expressions for the elements of the unit cell matrix:

$$\mathcal{M}_{11}^{(\text{cell})}(E) = [\cosh(\rho d) + i(E/\rho) \sinh(\rho d)]^2 + (m/\rho)^2 \exp(-2Q) \sinh^2(\rho d), \quad (8)$$

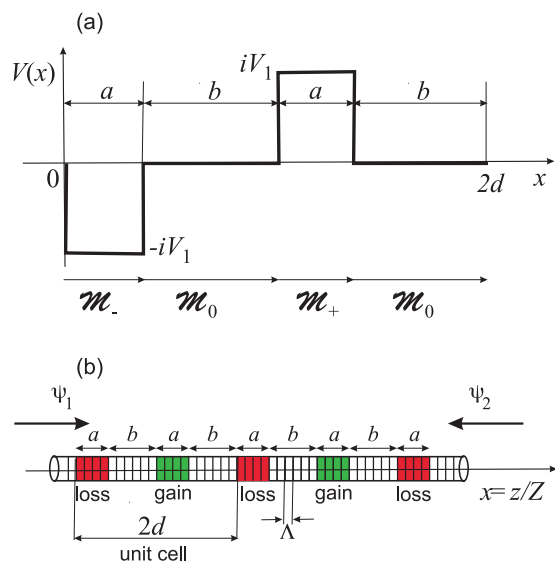


FIG. 1. (Color online) (a) Schematic behavior of the complex vector potential $V(x)$ in the unit cell for the \mathcal{PT} invariant DKP crystal and (b) its optical realization based on a superstructure FBG with alternating regions of gain and absorption. The 2×2 transfer matrix $\mathcal{M}^{(\text{cell})}$ of the unit cell, describing the propagation of the wave function ψ from $x = 0$ to $2d$, is obtained as the ordered product of the four matrices \mathcal{M}_- , \mathcal{M}_0 , \mathcal{M}_+ , and \mathcal{M}_0 shown in (a) and describing propagation in the four sections of the unit cell with $V(x)$ constant.

$$\mathcal{M}_{12}^{(\text{cell})}(E) = -\frac{2im \exp(Q)}{\rho} \sinh(\rho d) [\cosh(\rho d) \cosh(Q) + i(E/\rho) \sinh(\rho d) \sinh(Q)], \quad (9)$$

$$\mathcal{M}_{21}^{(\text{cell})}(E) = \frac{2im \exp(-Q)}{\rho} \sinh(\rho d) [\cosh(\rho d) \cosh(Q) + i(E/\rho) \sinh(\rho d) \sinh(Q)], \quad (10)$$

$$\mathcal{M}_{22}^{(\text{cell})}(E) = [\cosh(\rho d) - i(E/\rho) \sinh(\rho d)]^2 + (m/\rho)^2 \exp(2Q) \sinh^2(\rho d). \quad (11)$$

In the following we will focus our analysis mainly on the δ -Dirac limit of the potential wells and barriers.

B. Photonic realization

A physical realization of the \mathcal{PT} symmetric DKP Hamiltonian is provided by propagation and scattering of light waves in engineered superstructure fiber Bragg gratings (FBGs), or more generally in distributed-feedback optical structures with balanced optical gain and loss regions. Such optical structures have been recently shown to provide an accessible test bed to mimic in optics non-Hermitian relativistic quantum mechanics.²⁹ As compared to the photonic realization of the DKP with a *real* potential recently proposed in Ref. 7 and based on a superstructure FBG with a periodic sequence of π phase slips in the grating profile, in the \mathcal{PT} symmetric DKP model considered in the present work the *complex* potential $V(x)$ is realized by means of a periodic sequence of alternating regions of optical gain and absorption superimposed to the *uniform*

modulation of the refractive index [see Fig. 1(b)]. Hence the superstructure is obtained by superimposing to the primary (small-period Λ) index modulation a secondary (long-period $2d$) modulation of the gain/absorption. The formal analogy between light scattering in the superstructure FBG and the \mathcal{PT} invariant DKP model [Eq. (1)] can be established following the analysis of Ref. 29, which is here briefly reviewed for the sake of clearness. Let us consider propagation of a monochromatic optical wave at frequency ω in a one-dimensional periodic FBG with an effective refractive index profile

$$n(z) = n_0 - \Delta n m(z) \cos(2\pi z/\Lambda), \quad (12)$$

where n_0 is the modal refractive index in the absence of the grating, $\Delta n \ll n_0$ and Λ are the peak index change and the spatial period of the grating, respectively, and $m(z)$ is the normalized amplitude profile of the index grating. The periodic modulation of the refractive index leads to Bragg scattering between two counterpropagating waves at frequencies ω close to the Bragg frequency $\omega_B = \pi c/(\Lambda n_0)$, where c is the speed of light in vacuum. The optical fiber is assumed to include regions of optical gain and absorption, which can be realized by, e.g., rare-earth ion doping with optical pumping of the gain regions. The linear space-dependent gain coefficient of counterpropagating waves in the structure is indicated by $g(x)$ ($g < 0$ in the absorption regions, $g > 0$ in the gain regions).

Indicating by

$$\mathcal{E}(z) = \psi_1(z) \exp(i\pi z/\Lambda) + \psi_2(z) \exp(-i\pi z/\Lambda) \quad (13)$$

the spatial part of the electric field propagating in the fiber grating, the envelopes ψ_1 and ψ_2 of counterpropagating waves satisfy coupled-mode equations, which are obtained from the scalar Helmholtz equation by standard averaging or multiple-scale asymptotic methods (see, for instance, Refs. 6,29,33). After introduction of the normalized spatial variable $x = z/Z$ with the length scale Z defined by

$$Z = \frac{2n_0\Lambda}{\pi \Delta n}, \quad (14)$$

the coupled-mode equations take the form

$$E\psi_1 = -i \frac{d\psi_1}{dx} + m(x)\psi_2(x) + V(x)\psi_1(x), \quad (15)$$

$$E\psi_2 = i \frac{d\psi_2}{dx} + m(x)\psi_1(x) + V(x)\psi_2(x), \quad (16)$$

where $V(x)$ and E are given by

$$V(x) = iZg(x), \quad E = Z \left(\frac{\omega n_0}{c} - \frac{\pi}{\Lambda} \right). \quad (17)$$

In their present form, Eqs. (15) and (16) are formally analogous to the coupled equations for the two components ψ_1 and ψ_2 of the spinor wave function of the dimensionless Dirac Eq. (1) in the Weyl representation, in which the particle energy E and the (imaginary) vector potential $V(x)$ are defined by Eq. (17). Hence a periodic alternation of uniform regions of gain and absorption in the fiber realizes the complex potential of the DKP model, as shown in Fig. 1(b). Note that the δ -function limit of the DKP model corresponds to lumped regions of gain and absorption. In practice, this case is achieved whenever the physical length of the gain/loss regions is smaller than the characteristic length Z of optical feedback induced by the

grating [defined by Eq. (14)] and the gain/loss coefficient g is much larger than $1/Z$.

III. THE INFINITE CRYSTAL: BAND STRUCTURE AND \mathcal{PT} SYMMETRY BREAKING

In this section we consider the case of an infinite crystal and determine the band structure and the \mathcal{PT} symmetry breaking threshold of the DKP Hamiltonian \hat{H} . Owing to the periodicity of the potential $V(x)$, the eigenfunctions $\psi_E(x)$ of the Dirac Hamiltonian \hat{H} are of the Bloch-Floquet type; i.e., they satisfy the condition $\psi_E(x + 2d) = \psi_E(x) \exp(2ikd)$, where k is a real number (quasimomentum) that varies in the first Brillouin zone $-\pi/(2d) < k \leq \pi/(2d)$. The dispersion relation $E = E(k)$, which is generally a multivalued function, defines the band structure of the crystal. If complex energies do exist for some real quasimomentum k , the \mathcal{PT} phase is broken. At $Q = 0$, i.e., in the absence of the crystal, the energy spectrum of \hat{H} is real and composed by the positive and negative energy branches of the freely moving relativistic Dirac particle. As Q is increased from zero, complex energies do appear at some critical value $Q = Q_c$, which defines the \mathcal{PT} symmetry breaking point. As we will show below, for the DKP model one has $Q_c = 0$; i.e., the infinite complex crystal is always in the broken \mathcal{PT} phase.

The dispersion curve $E = E(k)$ of the various crystal bands can be determined in a standard manner by observing that, since $\psi_E(2d) = \mathcal{M}^{(\text{cell})}(E)\psi_E(0)$ and $\psi_E(2d) = \psi_E(0) \exp(2ikd)$, one has $\mathcal{M}^{(\text{cell})}(E)\psi_E(0) = \exp(2ikd)\psi_E(0)$; i.e., $\psi_E(0)$ is an eigenvector of $\mathcal{M}^{(\text{cell})}(E)$ with eigenvalue $\exp(2ikd)$. Taking into account that $\det \mathcal{M}^{(\text{cell})} = 1$, one then obtains

$$\exp(4ikd) - (\mathcal{M}_{11}^{(\text{cell})} + \mathcal{M}_{22}^{(\text{cell})}) \exp(2ikd) - 1 = 0. \quad (18)$$

After introduction of the complex angle $\theta = \theta(E)$ defined by $\cos \theta = \Delta(E)$, where the discriminant $\Delta(E)$ is defined as the semitrace of $\mathcal{M}^{(\text{cell})}(E)$,

$$\Delta(E) \equiv \frac{\mathcal{M}_{11}^{(\text{cell})} + \mathcal{M}_{22}^{(\text{cell})}}{2} = \frac{1}{2} \text{Tr}(\mathcal{M}^{(\text{cell})}), \quad (19)$$

one has $\exp(2ikd) = \exp(\pm i\theta)$, i.e.,

$$\cos(2kd) = \Delta(E). \quad (20)$$

Substitution of Eqs. (8) and (11) into Eq. (19) yields for the semitrace $\Delta(E)$ the explicit expression

$$\Delta(E) = \frac{m^2}{\rho^2} \cosh(2Q) \sinh^2(\rho d) + \cosh^2(\rho d) - \frac{E^2}{\rho^2} \sinh^2(\rho d), \quad (21)$$

where $\rho = (m^2 - E^2)^{1/2}$. Equations (20) and (21) implicitly define the dispersion curves $E = E(k)$ for the \mathcal{PT} invariant DKP crystal in the complex energy plane. The spectrum of \hat{H} is defined by the complex energies E such that $\Delta(E)$ is a real number and $-1 \leq \Delta(E) \leq 1$. Note that for $Q = 0$ Eq. (21) reduces to $\cos(2kd) = \cos(2d\sqrt{E^2 - m^2})$, which yields the two real energy branches $E = \pm\sqrt{m^2 + k^2}$ of the Dirac equation for a free particle. For $Q \neq 0$, the spectrum of \hat{H} can become complex. It can be readily shown that the \mathcal{PT}

phase of \hat{H} is broken at $Q_c = 0$, and that for an infinitesimally small value of the area Q of the δ -barrier complex energies emanate from the points

$$E_n = \pm\sqrt{m^2 + (\pi/2 + n\pi)^2/d^2} \quad (22)$$

on the real axis, with $n = 0, \pm 1, \pm 2, \dots$. To prove such a statement, let us consider the explicit form of the discriminant Δ , given by Eq. (21), as a function of both complex energy E and area Q of the δ barrier, and let us consider its asymptotic behavior by assuming $E = E_n + \delta E$, with δE small of order $\sim \epsilon$ and Q small of order $\sim \sqrt{\epsilon}$. The Taylor expansion of $\Delta(E, Q)$ around $E = E_n$ and $Q = 0$ yields

$$\Delta(E, Q) = \Delta^{(0)} + \epsilon \Delta^{(1)} + \epsilon^2 \Delta^{(2)} + o(\epsilon^3), \quad (23)$$

where we have set

$$\Delta^{(0)} = -1, \quad (24)$$

$$\Delta^{(1)} = \frac{2m^2 d^2 Q^2}{(\pi/2 + n\pi)^2}, \quad (25)$$

$$\Delta^{(2)} = \frac{4d^4 E_n^2 (\delta E)^2}{(\pi/2 + n\pi)^2} + \frac{2m^2 d^2 Q^4}{3(\pi/2 + n\pi)^2} - \frac{4Q^2 E_n d^4 \delta E}{(\pi/2 + n\pi)^4}. \quad (26)$$

Note that $\Delta^{(0)}$ and $\Delta^{(1)}$ are real numbers, with $\Delta^{(1)} > 0$, whereas $\Delta^{(2)}$ is in general a complex number. Indicating by δE_R and δE_I the real and imaginary parts of δE , respectively, let us choose δE_R such that $\Delta^{(2)}$ is a real number, i.e., $\delta E_R = Q^2/[2E_n(\pi/2 + n\pi)^2]$. In this case, for an arbitrary δE_I (of order $\sim \epsilon$), it turns out that $\Delta(E)$ at $E = E_n + \delta E_R + i\delta E_I$ is a real number and $|\Delta(E)| < 1$; i.e., E belongs to the spectrum of \hat{H} . This proves that, for an infinitesimal value of Q , complex energy branches emanate from the energies E_n on the real axis. Hence the \mathcal{PT} invariant DKP Hamiltonian is always in the broken \mathcal{PT} phase.

IV. THE FINITE CRYSTAL: SCATTERING PROPERTIES AND SPECTRAL SINGULARITIES

Let us consider a locally periodic crystal of finite length containing a finite number N of unit cells. In the optical realization discussed in Sec. II B, such a complex crystal is realized in a periodic grating of finite length $L = 2dNZ$. Owing to the boundary conditions that apply to the grating structure, we will assume $m(x) = 0$ [i.e., $S(x) = -m$] for $x < 0$ and $x > 2dN$. In this case, indicating by $\mathcal{M}(E) = [\mathcal{M}^{(\text{cell})}(E)]^N$ the transfer matrix that connects the spinor wave function $\psi(x)$ from the plane $x = 0$ to the plane $x = 2dN$ [i.e., $\psi(L) = \mathcal{M}(E)\psi(0)$], the transmission (t_N) and reflection (r_N) amplitude probabilities for left (L) and right (R) particle incidence are related to the elements of the transfer matrix \mathcal{M} by the simple relations (see, for instance, Ref. 29)

$$t_N^{(L)}(E) = t_N^{(R)}(E) \equiv t_N(E) = \frac{1}{\mathcal{M}_{22}}, \quad (27)$$

$$r_N^{(L)}(E) = -\frac{\mathcal{M}_{21}}{\mathcal{M}_{22}}, \quad r_N^{(R)}(E) = \frac{\mathcal{M}_{12}}{\mathcal{M}_{22}}. \quad (28)$$

Since $\mathcal{M}^{(\text{cell})}$ is a unimodular matrix, the transfer matrix $\mathcal{M} = [\mathcal{M}^{(\text{cell})}]^N$ can be calculated by means of the Cayley-Hamilton theorem according to Ref. 32:

$$\mathcal{M} = U_{N-1}(\cos \theta) \mathcal{M}^{(\text{cell})} - U_{N-2}(\cos \theta) \mathcal{I}, \quad (29)$$

where \mathcal{I} is the 2×2 identity matrix, $\cos \theta = \Delta(E)$ is the semitrace of $\mathcal{M}^{(\text{cell})}$ [see Eq. (19)], and $U_N(\xi)$ are the Chebychev polynomials of the second kind, defined by the recursion relation

$$U_{N+2}(\xi) - 2\xi U_{N+1}(\xi) + U_N(\xi) = 0, \quad (30)$$

with $U_0(\xi) = 1$ and $U_1(\xi) = 2\xi$. Chebychev polynomials of the second kind can be written in terms of sinusoidal functions,³² yielding

$$U_N(\cos \theta) = \frac{\sin[(N+1)\theta]}{\sin \theta}. \quad (31)$$

Using Eqs. (29) and (31) to compute the N th power of $\mathcal{M}^{(\text{cell})}$, the transmission and reflection probability amplitudes t_N and $r_N^{(L,R)}$ of the crystal made of N cells can be readily written in terms of the transmission and reflection coefficients t_1 and $r_1^{(L,R)}$ of the unit cell crystal as

$$t_N = \frac{t_1 \sin \theta}{\sin(N\theta) - t_1 \sin[(N-1)\theta]}, \quad (32)$$

$$r_N^{(L,R)} = \frac{\sin(N\theta)r_1^{(L,R)}}{\sin(N\theta) - \sin[(N-1)\theta]}. \quad (33)$$

Hence the scattering properties of the N -cell crystal can be simply calculated from the ones of the unit cell crystal using Eqs. (32) and (33). In the photonic realization of the DKP model discussed in Sec. II B, Eqs. (32) and (33) provide the transmission and reflection amplitudes of transmitted and reflected optical waves from the superstructure FBG shown in Fig. 1(b) when the grating is probed from the left or right sides with a monochromatic wave at frequency ω near the Bragg resonance frequency ω_B . For $Q = 0$, i.e., in the absence of the gain and loss regions, Eqs. (32) and (33) give the well-known relations of the transmission and reflection coefficients of a passive and periodic FBG of length $L = 2dNZ$ (see, for instance, Ref. 33), with $r_N^{(L)} = r_N^{(R)}$ and $|r_N^{(L,R)}|^2 + |t_N|^2 = 1$ owing to power conservation. In the presence of the gain and absorption regions, i.e., for $Q \neq 0$, the reflection probabilities (reflectance) $R_N^{(L,R)} = |r_N^{(L,R)}|^2$ for left- and right-side incidence are generally distinct, according to the general results of wave scattering from complex potential barriers,²⁶ and both reflectance $R_N^{(L,R)}$ and transmittance $T_N = |t_n|^2$ can be larger than one (owing to loss of unitarity). In particular, as Q is increased from zero, a critical value Q_c can be reached such that the transmission and reflection probabilities become singular at some real energy E_0 . At such a critical point, a resonance of \hat{H} crosses the real energy axis, and at $Q = Q_c^+$ a bound state with complex energy appears in the spectrum of \hat{H} ;²⁹ i.e., $Q = Q_c$ defines the \mathcal{PT} symmetry breaking point of the finite complex crystal. As discussed in previous works (see, for instance, Refs. 29 and 34 and references therein), at $Q = Q_c$ the Hamiltonian \hat{H} shows a spectral singularity at the energy $E = E_0$. The coexistence of spectral singularities and complex bound states as a signature of \mathcal{PT} symmetry breaking in nonrelativistic versions of \mathcal{PT} symmetric pairs of delta functions has been elucidated in Ref. 36. In our photonic realization of the DKP model, the onset of \mathcal{PT} symmetry breaking and the appearance of a spectral singularity correspond to the threshold for lasing of

the active FBG superstructure.^{29,35,37} Taking into account that $t_1 = 1/\mathcal{M}_{22}^{(\text{cell})}$, from Eq. (32) it follows that the \mathcal{PT} symmetry breaking point Q_c for the finite crystal can be calculated by imposing

$$\sin[(N-1)\theta] = \sin(N\theta)\mathcal{M}_{22}^{(\text{cell})}. \quad (34)$$

Using the expression of $\mathcal{M}_{22}^{(\text{cell})}$ given by Eq. (11), it can be readily shown that Eq. (34) can be satisfied at the energies E_n , defined by Eq. (22), provided that Q satisfies the nonlinear equation

$$\frac{m^2 d^2}{(\pi/2 + n\pi)^2} \sinh(2Q) = -\frac{\sin[\theta(Q)] \cos[N\theta(Q)]}{\sin[N\theta(Q)]}, \quad (35)$$

with

$$\theta(Q) = \text{acos} \left\{ -1 + \frac{m^2 d^2}{(\pi/2 + n\pi)^2} [\cosh(2Q) - 1] \right\}. \quad (36)$$

For an assigned value of the integer n , the roots of Eq. (35) can be numerically computed as the intersections of the two curves on the left- and right-hand sides of Eq. (35). Q_c is obtained as the smallest root to Eq. (35) when n is varied. Numerical analysis shows that, for a given value of n , Eq. (35) admits of a finite number of acceptable roots (Q real and $Q \geq 0$), and that the smallest root Q_c corresponds to the choice $n = 0$. From a physical viewpoint, $n = 0$ corresponds to the passive mode (resonance of \hat{H}) of the FBG superstructure with the lowest lasing threshold. An approximate expression of Q_c can be derived from Eqs. (35) and (36) by asymptotic expansions for small Q and $\theta \simeq \pi$, and reads

$$Q_c \simeq \frac{3}{4N} \left[\sqrt{1 + \frac{4}{3} \left(\frac{\pi}{2md} \right)^2} - 1 \right]. \quad (37)$$

As an example, Fig. 2 shows the \mathcal{PT} symmetry breaking value Q_c versus the number N of unit cells for $md = 1$ as obtained by numerical analysis of Eq. (35) (dots) and by the approximate relation (37) (continuous curve). Note that Q_c

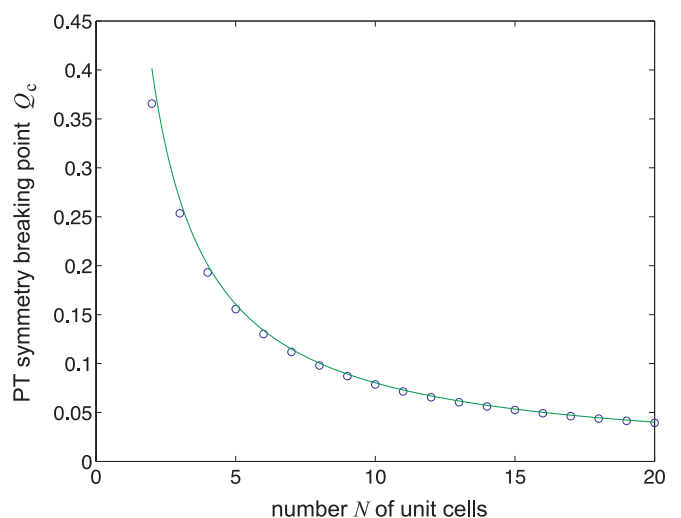


FIG. 2. (Color online) \mathcal{PT} symmetry breaking point Q_c of the finite DKP crystal for $md = 1$ and for increasing number N of unit cells (dots). The solid curve is the approximate value of Q_c as given by Eq. (37).

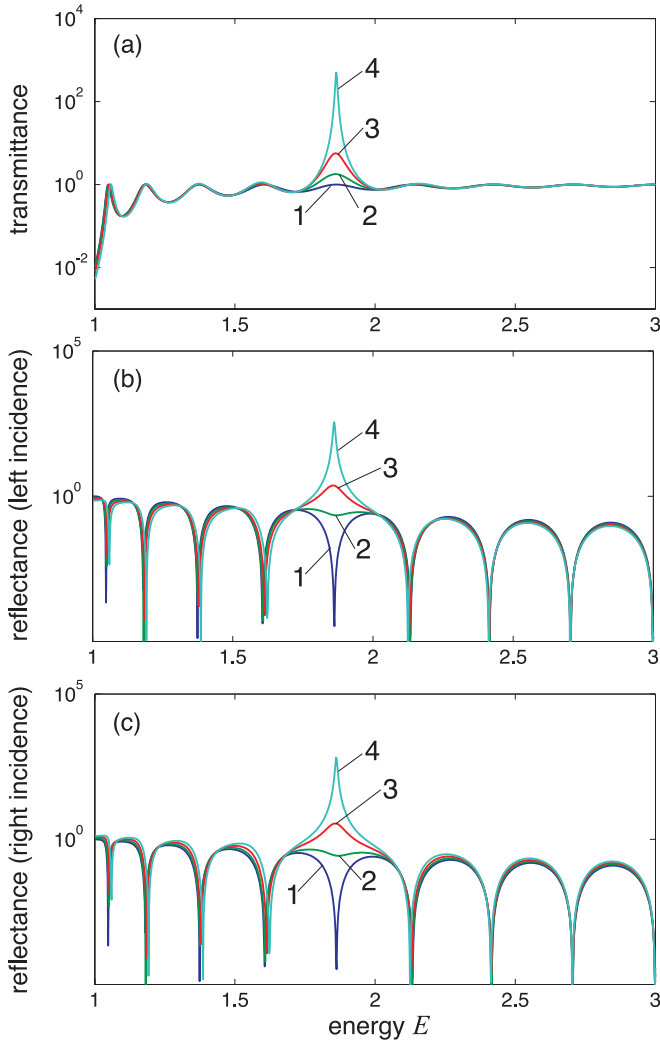


FIG. 3. (Color online) Behavior of (a) spectral transmittance and spectral reflectance for (b) left- and (c) right-side particle incidence in a \mathcal{PT} symmetric DKP crystal made of $N = 5$ unit cells for increasing values of Q and for $m = d = 1$. Curve 1: $Q = 0$; curve 2: $Q = 0.05$; curve 3: $Q = 0.1$; curve 4: $Q = 0.15$. The \mathcal{PT} symmetry breaking is attained at $Q_c \simeq 0.1556$.

goes to zero as $1/N$ for $N \rightarrow \infty$. Such a result is consistent with the analysis of Sec. III, in which we proved that the infinite DKP crystal is always in the broken \mathcal{PT} phase.

Typical examples of reflection and transmission probabilities in a finite crystal composed by $N = 5$ unit cells are depicted in Fig. 3 for increasing values of Q and for $m = d = 1$. The curves have been obtained using Eqs. (32) and (33), where the spectral transmission and reflection amplitude probabilities t_1 and $r_1^{(L,R)}$ of the unit cell crystal are computed using Eqs. ((8)–(10)) and ((27)–(28)). Note that, according to the previous analysis, a narrow and strong resonance peak does appear in the transmission and reflection spectra as Q approaches the \mathcal{PT} symmetry breaking value $Q_c \simeq 0.1556$ at the energy $E_0 = \sqrt{m^2 + \pi^2/(4d^2)} \simeq 1.862$.

It should be finally briefly mentioned that the previous analytical results hold for the δ -Dirac limit of the potential barriers and wells in the comb, however similar results are obtained by assuming a rectangular shape for the barriers and

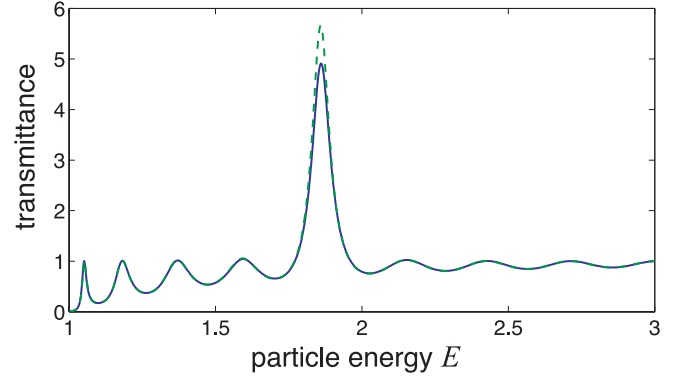


FIG. 4. (Color online) Behavior of spectral transmittance (solid curve), numerically computed using Eqs. ((3)–(5)), in a crystal composed by $N = 5$ cells for parameter values $m = 1$, $d = 1$, $a = 0.2$, and $V_1 = 0.5$. The dashed curve depicts the behavior of the spectral transmittance as computed for the δ -Dirac limit of the potential wells and barriers with an area $Q = V_1 a = 0.1$.

wells with a finite length a [see Fig. 1(a)]. As an example, Fig. 4 shows the numerically computed transmission probability for a crystal composed of $N = 5$ unit cells for $d = 1$, $a = 0.2$, and $V_1 = 0.5$. In the same figure, the curve corresponding to the δ -Dirac limit of the DKP crystal, with $S = V_1 a = 0.1$, is also depicted for comparison. The main effect of a finite length a is the introduction of a small shift in the onset of \mathcal{PT} symmetry breaking, i.e., in the lasing threshold of the superstructure FBG. In the photonic realization discussed in Sec. II B, assuming a FBG at the wavelength $\lambda_B \simeq 1.55 \mu\text{m}$ of optical communications, a typical index change $\Delta n = 0.5 \times 10^{-4}$ and refractive index $n_0 = 1.5$ of the fiber,⁶ the grating period Λ turns out to be $\Lambda = \lambda_B/(2n_0) \simeq 516.7 \text{ nm}$. Correspondingly, the characteristic spatial length Z , defined by Eq. (14), turns out to be $Z \simeq 9.87 \text{ mm}$. Hence the physical grating length corresponding to the simulation of Fig. 4 is $L = 2dNZ = 9.87 \text{ cm}$, the length of gain/absorption regions is $Za = 1.97 \text{ mm}$, and the gain/absorption coefficient is [see Eq. (17)] $\hat{E}g = V_1/Z \simeq 0.5 \text{ cm}^{-1} \simeq 4.34 \text{ dB/cm}$. Such levels of gain/absorption can be achieved using erbium-doped phosphate fibers³⁸ or glass waveguides³⁹ at high doping concentrations.

V. CONCLUSIONS

In this work we have introduced a complex extension of the Dirac-Kronig-Penney model for a \mathcal{PT} symmetric crystal describing the dynamics of Dirac quasiparticles in a periodic sequence of alternating imaginary δ -Dirac barriers and wells, and investigated analytically the onset of \mathcal{PT} symmetry breaking for both the infinite crystal and the finite crystal as the number N of cells is increased. The main result of our analysis is that the \mathcal{PT} phase is unbroken below a finite threshold of the δ -barrier area which scales as $\sim 1/N$. Hence for the infinitely long crystal the \mathcal{PT} phase is always broken, a result which is different from, e.g., the symmetry breaking properties of other exactly solvable models (like the sinusoidal \mathcal{PT} symmetric crystal^{19,20}). A perturbative analysis of the band dispersion curve of the infinite crystal shows that the broken \mathcal{PT} phase is associated with a countable number of

complex energy branches that emanate from the positive and negative energy branches of the freely moving Dirac particle.

Our complex extension of the standard Kronig-Penney model of solid-state physics can find applications in scattering problems of optical or matter waves from complex optical potentials, and can motivate further theoretical and experimental investigations of the scattering and transport properties of complex crystals. For example, an extension of the complex DKP model presented in this work to two-dimensional honeycomb lattices with superimposed gain and loss regions

could be of interest in the study of the scattering and transport properties of relativistic quasiparticles in graphenelike systems with superimposed complex potential wells and barriers.

ACKNOWLEDGMENTS

S.L. acknowledges financial support by the Italian Ministero dell' 'Istruzione, dell' Univerità e della Ricerca (Grant No. PRIN-2008-YCAAK, project "Analogie ottico-quantistiche in strutture fotoniche a guida d'onda").

-
- ¹R. de L. Kronig and W. G. Penney, *Proc. R. Soc. London A* **130**, 499 (1931).
- ²F. Dominguez-Adame, *Am. J. Phys.* **55**, 1003 (1987).
- ³S. G. Davison and M. Streslicka, *J. Phys. C* **2**, 1802 (1969); B. H. J. McKellar and G. J. Stephenson, *Phys. Rev. A* **36**, 2566 (1987); F. Dominguez-Adame, *J. Phys. Condens. Matter* **1**, 109 (1989); C. L. Roy and C. Basu, *J. Phys. Chem. Solids* **52**, 745 (1991); F. Dominguez-Adame and A. Sanchez, *Phys. Lett. A* **159**, 153 (1991).
- ⁴G. J. Clerk and B. H. J. McKellar, *Phys. Rev. C* **41**, 1198 (1990).
- ⁵G. J. Clerk and B. H. J. McKellar, *Phys. Rev. B* **47**, 6942 (1993); C. Basu, C. L. Roy, E. Macia, F. Dominguez-Adame, and A. Sanchez, *J. Phys. A* **27**, 3285 (1994); F. Dominguez-Adame, E. Macia, A. Khan, and C. L. Roy, *Physica B* **212**, 67 (1995); M. Barbier, F. M. Peeters, P. Vasilopoulos, and J. M. Pereira, *Phys. Rev. B* **77**, 115446 (2008).
- ⁶D. Janner, G. Galzerano, G. Della Valle, P. Laporta, S. Longhi, and M. Belmonte, *Phys. Rev. E* **72**, 056605 (2005); S. Longhi, D. Janner, G. Galzerano, G. Della Valle, D. Gatti, and P. Laporta, *Electron. Lett.* **41**, 1075 (2005).
- ⁷S. Longhi, *Cent. Eur. J. Phys.* **9**, 110 (2011); *Appl. Phys. B* **104**, 453 (2011).
- ⁸G. W. Semenoff, *Phys. Rev. Lett.* **53**, 2449 (1984).
- ⁹K. S. Novoselov *et al.*, *Nature (London)* **438**, 197 (2005); Y. Zhang *et al.*, *ibid.* **438**, 201 (2005).
- ¹⁰S. L. Zhu, B. Wang, and L. M. Duan, *Phys. Rev. Lett.* **98**, 260402 (2007); C. Chamon, C. Yu Hou, R. Jackiw, C. Mudry, S.-Y. Pi, and G. Semenoff, *Phys. Rev. B* **77**, 235431 (2008); C. Wu and S. Das Sarma, *ibid.* **77**, 235107 (2008); I. I. Satija, D. C. Dakin, J. Y. Vaishnav, and C. W. Clark, *Phys. Rev. A* **77**, 043410 (2008); J. Ruostekoski, J. Javanainen, and G. V. Dunne, *ibid.* **77**, 013603 (2008).
- ¹¹J. Ruseckas, G. Juzeliunas, P. Öhberg, and M. Fleischhauer, *Phys. Rev. Lett.* **95**, 010404 (2005); S.-L. Zhu, H. Fu, C.-J. Wu, S.-C. Zhang, and L.-M. Duan, *ibid.* **97**, 240401 (2006); X.-J. Liu, X. Liu, L. C. Kwek, and C. H. Oh, *ibid.* **98**, 026602 (2007); T. D. Stanescu, C. Zhang, and V. Galitski, *ibid.* **99**, 110403 (2007); J. Y. Vaishnav and C. W. Clark, *ibid.* **100**, 153002 (2008).
- ¹²L. Lamata, J. Leon, T. Schatz, and E. Solano, *Phys. Rev. Lett.* **98**, 253005 (2007); R. Gerritsma, G. Kirchmair, F. Zähringer, E. Solano, R. Blatt, and C. F. Roos, *Nature (London)* **463**, 68 (2010); R. Gerritsma, B. P. Lanyon, G. Kirchmair, F. Zähringer, C. Hempel, J. Casanova, J. J. Garcia-Ripoll, E. Solano, R. Blatt, and C. F. Roos, *Phys. Rev. Lett.* **106**, 060503 (2011).
- ¹³O. Peleg, G. Bartal, B. Freedman, O. Manela, M. Segev, and D. N. Christodoulides, *Phys. Rev. Lett.* **98**, 103901 (2007); X. Zhang, *ibid.* **100**, 113903 (2008); O. Bahat-Treidel, O. Peleg, M. Grobman, N. Shapira, M. Segev, and T. Pereg-Barnea, *ibid.* **104**, 063901 (2010).
- ¹⁴A. Szameit, M. C. Rechtsman, O. Bahat-Treidel, and M. Segev, *Phys. Rev. A* **84**, 021806 (2011).
- ¹⁵M. Barbier, P. Vasilopoulos, and F. M. Peeters, *Phys. Rev. B* **80**, 205415 (2009); S. Gattenlöhner, W. Belzig, and M. Titov, *ibid.* **82**, 155417 (2010); M. Ramezani Masir, P. Vasilopoulos, and F. M. Peeters, *J. Phys. Condens. Matter* **22**, 465302 (2010); M. Barbier, P. Vasilopoulos, and F. M. Peeters, *Phys. Rev. B* **82**, 235408 (2010); C. H. Pham, H. C. Nguyen, and V. L. Nguyen, *J. Phys. Condens. Matter* **22**, 425501 (2010).
- ¹⁶F. Cannata, G. Junker, and J. Trost, *Phys. Lett. A* **246**, 219 (1998); C. M. Bender, G. V. Dunne, and P. N. Meisinger, *ibid.* **252**, 272 (1999); J. M. Cervero, *ibid.* **A317**, 26 (2003); K. C. Shin, *J. Phys. A: Math. Gen.* **37**, 8287 (2004).
- ¹⁷Z. Ahmed, *Phys. Lett. A* **286**, 231 (2001).
- ¹⁸C. Keller, M. K. Oberthaler, R. Abfalterer, S. Bernet, J. Schmiedmayer, and A. Zeilinger, *Phys. Rev. Lett.* **79**, 3327 (1997); M. V. Berry, *J. Phys. A* **31**, 3493 (1998); M. V. Berry and D. H. J. O'Dell, *ibid.* **31**, 2093 (1998).
- ¹⁹K. G. Makris, R. El-Ganainy, D. N. Christodoulides, and Z. H. Musslimani, *Phys. Rev. Lett.* **100**, 103904 (2008); Z. H. Musslimani, K. G. Makris, R. El-Ganainy, and D. N. Christodoulides, *ibid.* **100**, 030402 (2008); K. G. Makris, R. El-Ganainy, D. N. Christodoulides, and Z. H. Musslimani, *Phys. Rev. A* **81**, 063807 (2010); M. C. Zheng, D. N. Christodoulides, R. Fleischmann, and T. Kottos, *ibid.* **82**, 010103 (2010).
- ²⁰S. Longhi, *Phys. Rev. A* **81**, 022102 (2010); E.-M. Graefe and H. F. Jones, *ibid.* **84**, 013818 (2011).
- ²¹S. Longhi, *Phys. Rev. Lett.* **103**, 123601 (2009); *Phys. Rev. B* **80**, 235102 (2009).
- ²²O. Bendix, R. Fleischmann, T. Kottos, and B. Shapiro, *Phys. Rev. Lett.* **103**, 030402 (2009); L. Jin and Z. Song, *Phys. Rev. A* **80**, 052107 (2009); C. Hao Chang, S.-M. Wang, and T.-M. Hong, *ibid.* **80**, 042105 (2009); G. L. Giorgi, *Phys. Rev. B* **82**, 052404 (2010); Y. N. Joglekar, D. Scott, M. Babbey, and A. Saxena, *Phys. Rev. A* **82**, 030103 (2010); A. E. Miroshnichenko, B. A. Malomed, and Y. S. Kivshar, *ibid.* **84**, 012123 (2011); S. V. Dmitriev, S. V. Suchkov, A. A. Sukhorukov, and Yuri S. Kivshar, *ibid.* **84**, 013833 (2011); D. D. Scott and Y. N. Joglekar, *ibid.* **83**, 050102 (2011).
- ²³Z. Lin, H. Ramezani, T. Eichelkraut, T. Kottos, H. Cao, and D. N. Christodoulides, *Phys. Rev. Lett.* **106**, 213901 (2011); S. Longhi, *J. Phys. A: Math. Theor.* **44**, 485302 (2011).

- ²⁴C. M. Bender and S. Boettcher, *Phys. Rev. Lett.* **80**, 5243 (1998); C. M. Bender, *Rep. Prog. Phys.* **70**, 947 (2007); A. Mostafazadeh, *Phys. Scr.* **82**, 038110 (2010).
- ²⁵C. E. Rüter, K. G. Makris, R. El-Ganainy, D. N. Christodoulides, M. Segev, and D. Kip, *Nat. Phys.* **6**, 192 (2010).
- ²⁶Z. Ahmed, *Phys. Rev. A* **64**, 042716 (2001); F. Cannata, J.-P. Dedonder, and A. Ventura, *Ann. Phys.* **322**, 397 (2007); F. Cannata and A. Ventura, *J. Phys. A: Math. Theor.* **43**, 075305 (2010).
- ²⁷S. V. Dmitriev, A. A. Sukhorukov, and Y. S. Kivshar, *Opt. Lett.* **35**, 2976 (2010).
- ²⁸M. C. Zheng, D. N. Christodoulides, R. Fleischmann, and T. Kottos, *Phys. Rev. A* **82**, 010103 (2010).
- ²⁹S. Longhi, *Phys. Rev. Lett.* **105**, 013903 (2010).
- ³⁰F. Cannata and A. Ventura, *Phys. Lett. A* **372**, 941 (2008).
- ³¹B. H. J. McKellar and G. J. Stephenson Jr., *Phys. Rev. C* **35**, 2262 (1987).
- ³²D. J. Griffiths and C. A. Steinke, *Am. J. Phys.* **69**, 137 (2001).
- ³³T. Erdogan, *J. Lightwave Technol.* **15**, 1277 (1997).
- ³⁴A. Mostafazadeh, *Phys. Rev. Lett.* **102**, 220402 (2009).
- ³⁵S. Longhi, *Phys. Rev. A* **82**, 031801 (2010).
- ³⁶A. Mostafazadeh and H. Mehri-Dehnavi, *J. Phys. A: Math. Theor.* **42**, 125303 (2009).
- ³⁷A. Mostafazadeh, *Phys. Rev. A* **83**, 045801 (2011); **84**, 023809 (2011).
- ³⁸B. Hwang, S. Jiang, T. Luo, K. Seneschal, G. Sorbello, M. Morrell, F. Smektala, S. Honkanen, J. Lucas, and N. Peyghambarian, *IEEE Photonics Technol. Lett.* **13**, 197 (2001).
- ³⁹S. F. Wong, E. Y. B. Pun, and P. S. Chung, *IEEE Photonics Technol. Lett.* **14**, 80 (2002).